10th World Congress on Structural and Multidisciplinary Optimization
May 19 -24, 2013, Orlando, Florida, USA

Design Exploration of Robust Topologies under the Loading Uncertainty for the Lug Structure of Super Sonic Transportation

Hyunjin Shin[1], Yoshiyasu Hirano[2], Akira Todoroki[1]

[1] Department of Mechanical Sciences and Engineering, Tokyo Institute of Technology, Tokyo, JAPAN, hshin@ginza.mes.titech.ac.jp, atodorok@ginza.mes.titech.ac.jp
[2] Japan Aerospace Exploration Agency, Mitaka-city, Tokyo, JAPAN, hirano.yoshiyasu@jaxa.jp

1. Abstract
In Super Sonic Transportation (SST), thin wing structure is necessary to satisfy the high speed, economic viability and environmental compatibility requirements. Among many structures in thin wing, the lug structure which is between the body and the main wing plays important role. However, it is difficult to design the lug structure because it is subjected many loads that have uncertainties such as magnitude or direction of loading caused by aeroelastic forces. Robust topology optimization is, therefore, necessary to determine the optimal structural lay out solutions insensitive to loading uncertainties for design of the lug structure. The present paper proposes a method to explore robust topologies in Pareto-solutions of topology optimization problem with multi-loadcase. Pareto-solutions are obtained by using NSGA-IIa algorithm which is one of the most popular in Multi-Objective Evolutionary Algorithms (MOEA). In proposed method, Monte Carlo simulations were used to estimate the robustness of topology from Pareto optima obtained with NSGA-IIa. The obtained robust topology solutions are explored by Self-Organizing Map that is an appropriate tool to visualize and explore properties of the high dimension data such as topology. Finally, proposed method approach is applied for the lug structure robust topology optimization.
2. Keywords: Topology optimization, Multi-objective Genetic Algorithm, Self-Organizing Map, Data-Mining

3. Introduction
In order to satisfy the high speed, economic viability and environmental compatibility requirements, a thin wing structure plays a key role in the Super Sonic Transportation (SST). In general, it is difficult to apply the torque box structure that is usually used subsonic airplane to SST, because SST has not enough space. Instead of torque box structure, a lug structure that connects the body and the main wing is necessary with the multi-spar structure. Since lug structure is subjected to many loadings that have uncertainty such as magnitude and direction of loading caused by aeroelastic forces, design to account for uncertainty should thus be employed.

Topology optimization was used this kind of structure design problem to find the optimal structure lay-out within a design domain. However, if there is no considering loading uncertainty in topology optimization, optimal solutions may be unstable even under small loading uncertainty [1]. For the loading uncertainties, several robust topology optimization approaches have been proposed, for instance, worst case design [1] and methods for approximating probabilistic uncertainties to calculate expected performance [2], [3]. These approaches usually transform probabilistic problem into the multi-loadcase model. After that, robust optimization with multi-loadcase model is optimized using a minimax method or the expected compliance model. These approaches basically based on the compliance minimization problem of the multi-loadcase. This implies that a robust solution is the part of the Pareto-solutions of the multi-loadcase problem. Thus, in this study, robust topology is explored in the Pareto-solutions obtained from the compliance minimization problem of the multi-loadcase. In the present study, the elitist non-dominated sorting genetic algorithms (NSGA-IIa) that is powerful for multi-objective optimization problem was used to get Pareto-solutions.

However, if there are one more uncertainty loadings in a structure such as lug structure mentioned above, there may be exist one more robust topology solution. In that case, it is important to determine the final robust solution from many candidates such as Pareto-solutions. It is also necessary that some useful information is adequately provided to explore the final decision. In robust topology optimization problem, relations between topology and each loadcase, as well as trade-off relations between each loadcase and robustness performance are useful information. This information will be useful to understand some characteristics of each robust topology.

This paper focuses on robust topology exploration method in the Pareto-solutions of the multi-loadcase problem obtained by Multi-Objective Evolutionary Algorithms (MOEA). For the exploration, we used the Self-Organizing Map (SOM) [4] which is a nonlinear projection algorithm for multi-dimensional numerical data. By using SOM, we can effectively visualize and explore some relations that exist in the robust topology optimization problem. On the other hand, for estimation of the robustness of topology from Pareto-solutions, Monte-Carlo simulation was used, but it is require many times of FEM evaluations to get an accuracy of the

simulation. In order to reduce the computational cost, Kriging surrogate model [5] was used.

Finally, proposed approach was applied to a lug structure of SST for the robust topology optimization. Topology of the lug structure, which is subjected to bending moment and shear force with some loading uncertainty, was optimized to minimize the compliance of each loadcase with a volume constraint. After that, exploration of robust topology was conducted on the SOM.

4. Proposed method of exploration of robust topologies

In present study, Pareto-solutions of the compliance minimization problem of the multi-load case were obtained by using NSGA-IIa [6], [7]. After that, robust topology solutions were explored using SOM in the Pareto-solutions obtained by NSGA-IIa. Procedure of the proposed method is as follows.

1) Define load cases by considering uncertainties of loads.
2) Implement the NSGA-IIa for minimize-compliance problem with the multi-load case.
3) Classify the Pareto-solutions of the multi-load case problem according to topological characteristics of the Pareto-solutions by SOM.
4) Select the representative topologies from SOM.
5) Calculate the expected compliance and standard deviation of compliance for evaluation of robustness. In this step, Kriging surrogate model was used in order to reducing calculation cost.
6) Explore the robust topology on the SOM.

Monte Carlo simulation of the step 5 is high computational cost. It is inefficient to calculate the robustness performance of all Pareto solutions. Representative topology of each SOM unit, therefore, was extracted to reduce computational cost, since topologies in the same SOM unit are almost similar each other.

4.1. Loadcase with considering the loading uncertainty

In this study, to simulate the uncertainty in the loading direction, three-levels direction loads were considered, for instance, load cases whose direction of loadings are $\mu_D°$, $\mu_D \pm S \cdot \sigma_D°$, where μ_D is mean direction, σ_D is standard deviation of uncertain loading and S is the constant.

For verification of the three-levels direction loadcase, two examples were introduced as follows. In example 1, loading *f1* has mean applied direction $\mu_D = 0°$ and standard deviation $\sigma_D = 2.5°$. To find critical loadcase and levels, expected compliance of five cases (S = 0.4, 1, 2, 3, 4, 6) using three-levels and one case (S = [0, 1, 2]) using five-levels were compared on example1. In example 2, loading *f2* has the mean applied direction $\mu_D = -45°$ and standard deviation $\sigma_D = 40°$. To find critical loadcase and levels, expected compliance of six cases (S=0.25, 0.5, 1, 1.5, 5, 2.25) using three-levels and one case using 15-levels were compared on example2. Applied direction of each loadcase defined in examples 1, 2 is shown Table. 1. Here, for expected compliance calculation of each case, all Pareto-solutions obtained by NSGA-IIa are evaluated using Monte-Carlo simulation with Kriging model.

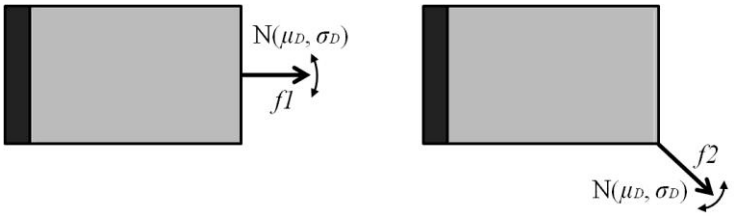

(a) Loading f1 with uncertainty N(0°,2.5°) (b) Loading f2 with uncertainty N(-45°,40°)

Figure 1: Two examples of the cantilever beam

Table 1: Loadcases of each example

Level	CASE	Example 1		Example 2	
		Degree	S	Degree	S
3 levels	CASE1	0, ±1	0.4	-55, -45, -35	0.25
	CASE2	0, ±2.5	1	-65, -45, -25	0.5
	CASE3	0, ±5	2	-85, -45, -5	1
	CASE4	0, ±7.5	3	-105, -45, 15	1.5
	CASE5	0, ±10	4	-125, -45, 35	2
	CASE6	0, ±15	6	-135, -45, 45	2.25
Multi-levels	CASE7	0, ±2.5, ±5	1, 2	-145, -125, -105, -85, -65, -55, -45, -35, -25, -5, 15, 35, 55	0.25, 0.5, 1, 1.5, 2, 2.5

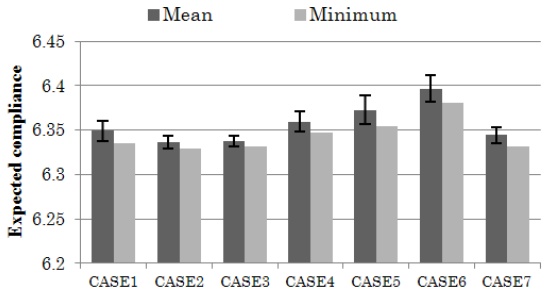

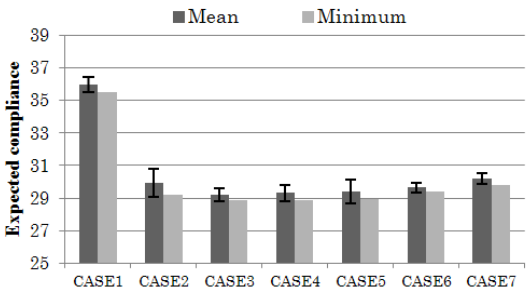

(a) Result of example 1 (b) Result of example 2

Figure 2: Comparison of expected compliance value

Expected compliance results of each example are shown in Fig.2. We can find that case of 3-levels with S=1 has a most minimum expected compliance in both examples. It is interesting to note that although multi-levels case objective space is much bigger than 3-levels objective space, as well as it contains the 3-levels objective space, expected compliance of 3-levels case with S=1 is less than multi-levels case result in both example. We thought that obtained result of multi-levels case was local optimum point. However, even though global optimum solution of the multi-levels case is obtained, there is not much difference in expected compliance value between multi-levels and 3 levels case. This result means that 3 levels loadcases with S=1 is enough to explore robust topologies. In present study, 3 levels loadcases with S=1 are used.

4.2. Multi-Objective topology optimization with Bar-system representation method

It is very important of the choice of the representation method of topology in the Genetic Algorithms. Among several representation methods, Bar-representation method [8] was used in the present study. Bar-representation method uses a series of bars between loads and support region in the design domain to represent a topology of structure. Thus this representation method maintains the proper connectivity of topology in the process of GA, so generation of improper connectivity topology can be suppressed. In this representation method, each vertices position and edges thickness of the bar was used for parameters for design problem. For mapping into the finite element mesh, if the center of gravity of element lies under the bars, 1 is given to the element density.

For minimization of the compliance in the multi-loadcase problem, the elitist non-dominated sorting genetic algorithms (NSGA-IIa) [6], [7] which is one of the most established Multi-Objective Evolutionary algorithms was used. A flow of this algorithm is similar to the common genetic algorithms. However in order to improve diversity and convergence of solutions, the crowding distance are calculated and a selection based on crowding distance called the crowded tournament selection was used in NSGA-IIa. Crowding distance is the relative distance to other solutions in the objective space. In addition, elitist strategy was applied to avoid problem of losing Pareto-optimal solutions when the number of the Pareto-solutions of algorithm exceeds the population size. In this present study, archiving method was used for elitist strategy [7]. For crossover method, Parent Centric crossover (PCX) [9] and Binary like crossover method was used simultaneously, and for mutation method, Polynomial mutation [10] was used.

In the Multi-Objective Optimization Problem, minimization of the compliance of p loadcase problem can be formulated in a discrete form as follows:

$$\begin{aligned} &\text{Minimize} : \mathbf{f}_k^T \mathbf{u}_k \quad k = 1,..., \text{p} \\ &s.t\ \mathbf{K}(x)\mathbf{u}_k = \mathbf{f}_k \ \text{for all}\ k = 1,..., \text{p}, \\ &\int_\Omega d\Omega \le \text{Volume limit} \end{aligned} \tag{1}$$

where Ω is the design domain, $\mathbf{f}_k$ is the force matrix of k loadcase, $\mathbf{u}_k$ is the k displacement matrix, $\mathbf{K}$ is the stiffness matrix.

4.3. Classification using Self-Organizing Map and extraction of representative topologies

For the efficient exploration and extraction the representative topologies from the Pareto-solutions obtained by NSGA-IIa, Self-Organizing Map (SOM) was used. SOM is the one of the artificial neural network algorithms using unsupervised learning. It is useful for visualizing the low dimensional views of high dimensional data. Therefore it is proper to classify the high dimensional data such as topology, and find some relations between data set by the visualization of data space.

The SOM consists of a 2 dimensional regular grid of map units. Each unit (neuron) i is associated with prototype vector $\mathbf{m}=[m_{i1},\cdots,m_{id}]$, where d is dimension of the input vector. Each unit has neighborhood relation

with its adjacent units. Input vectors have high relations each other in the input space are mapped onto nearby unit on the SOM. Thus, after mapping to the SOM, it can preserve the relation in the high dimensional space.

The learning algorithm of the SOM is trained iteratively. On each training step, a sample data $\boldsymbol{x}_S$ chosen from the input vectors is selected, and find the nearest unit from the map by calculating the distance between a sample $\boldsymbol{x}_S$ and all the prototype vectors. Nearest unit called Best Matching Unit(BMU) $\boldsymbol{m}_C$ is calculated as follows.

$$\|x_S - m_C\| = \min_i \{\|x_s - m_i\|\} \tag{2}$$

Next, the prototype vectors of the BMU and its neighbors are updated to move closer the sample vector.

For the classification of various topologies in the Pareto-solutions obtained NSGA-IIa, below topology characteristics are defined and used for the input data of SOM classification. Examples of the topology images that are some solutions of 2 loadcases problem optimized by MOEA are presented Fig. 3. As shown Fig. 3, if we don`t use some statistical features of the density distribution, it is difficult to classify these topologies.

- Feature1: All elements density value of the Finite Element Analysis model.
- Feature2: The width and height, in element that density is 1, of the FEA model.
- Feature3: The mean of the density of FEA element about each axis.
- Feature4: The variance of the density of FEA element about each axis.
- Feature5: The covariance of the density of FEA element about each axis.

These characteristics of topology are extracted from Pareto solutions, and then Pareto solutions are classified on the 2-dimensional SOM according to topology similarity as defined above.

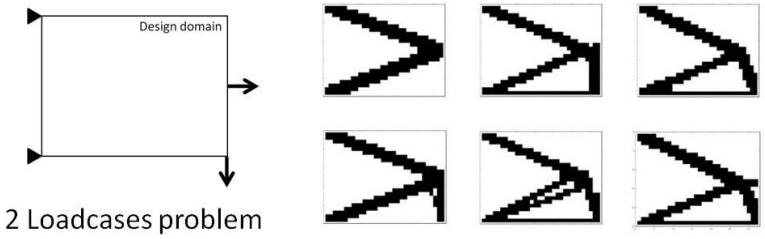

Figure 3: Examples of the topology images generated by MOEA

In the present study, representative topologies of the Pareto solutions are extracted on the SOM for efficiency of the Monte Carlo simulation. In the classification of SOM, input vectors which have a higher degree of similarity than others are mapped onto same unit on the SOM as shown in Fig. 4.

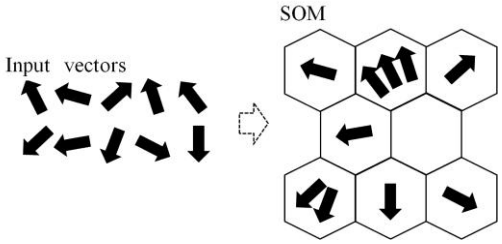

Figure 4: Illustration of classification using SOM

If there are several similar topologies in the certain unit of SOM, one topology is selected randomly, and then selected topology is set as the representative topology of the unit. After determining representative topology of all unit, selected topologies are calculated the expected compliance and the variance of compliance using Monte Carlo simulation. In the present study, SOM Toolbox package [11] for Matlab® was used for the classification of topologies.

In addition, to obtain useful information from the classification, it is necessary to select the interesting group of map units from the SOM, not all map units individually, for an efficient data mining. Thus, it is highly recommended to determine the good candidate for map unit clusters or groups for effective utilization of the information of SOM. In the present study, k-means clustering method [12] that is robust and visually efficient was used for clustering on the SOM. In the k-means clustering method, a data set is divided into a number of clusters by using an error function as follows.

$$E = \sum_{k=1}^{C} \sum_{x \in Q_k} \|x - c_k\|^2 \tag{3}$$

where C is the number of cluster, Q_k, $\boldsymbol{c}_k$ represent the set of cluster k and the center of cluster k, respectively.

4.4. Kriging surrogate model for Monte Carlo simulation

In this study, Kriging surrogate model was constructed to approximate the expectation and variance of compliance for efficient Monte Carlo simulation. Kriging model is the stochastic interpolating method developed in the field of spatial statistics and geostatistics. In Kriging method, there is several type of Kriging according to its statistic model. In this study, DACE (Design Analysis of Computer Experiments) model was used. DACE model has a feature that response surface passes through the sample points. This is suitable to approximate the data calculated by FEM analysis because the data has no experimental error.

Prediction of a response value y is defined as following equation in Kriging method.

$$\hat{y}(\mathbf{x}) = \mu(\mathbf{x}) + Z(\mathbf{x}) \tag{4}$$

where x is a vector of design variables, μ is the global model and Z is a deviation from the mean. The correlation between $Z(x^i)$ and $Z(x^j)$ is strongly depend on distance between x^i and x^j. Correlation function between any two points x^i and x^j is defined in the form of Gaussian correlation function as follows.

$$R(x^i, x^j) = \exp[-\sum_{m=1}^{k} \eta_m \left| x^{im} - x^{jm} \right|^2 \tag{5}$$

where k is the number of design variables, η is Kriging parameter, and x^{im} and x^{jm} are mth element of vector x^i and x^j respectively. The predictor of y at design point x is express as follows.

$$\hat{y}(\mathbf{x}) = \hat{\mu} + \mathbf{r}^T(\mathbf{x})\mathbf{R}^{-1}(\mathbf{y} - \mathbf{1}\hat{\mu}) \tag{6}$$

where r is a column vector, each element of which corresponds to a correlation function between predicting point x and sample point x^i, R is k × k matrix, each element of which correspond to a correlation function $R(x^i, x^j)$, and y is the column vector of response value of sample points. $\hat{\mu}$ is a predictor of μ, which is calculated as bellow.

$$\hat{\mu} = \frac{\mathbf{1}^T \mathbf{R}^{-1} \mathbf{y}}{\mathbf{1}^T \mathbf{R}^{-1} \mathbf{1}} \tag{7}$$

variance of $\hat{\mu}$ is calculated as

$$\hat{\sigma}^2 = \frac{(\mathbf{y} - \mathbf{1}\hat{\mu})^T \mathbf{R}^{-1} (\mathbf{y} - \mathbf{1}\hat{\mu})}{n} \tag{8}$$

Estimating a Kriging model is equal to determine Kriging parameters that maximize the following likelihood function.

$$Ln(\boldsymbol{\eta}) = -\left[n \ln\left(\hat{\sigma}^2(\boldsymbol{\eta})\right) + \ln|\mathbf{R}| \right] / 2 \tag{9}$$

In this presented study, in order to improve expected compliance and standard deviation, Kriging model was used to approximate the compliance space of each topology, and design variable in the Kriging model are magnitude and direction of force.

5. Exploration of the robust topology for lug structure

The proposed method in this present study was applied to the robust topology optimization problem of the lug structure. In the proposed method, since there are the expected compliance and standard deviation (or variance) of compliance model as robustness performance for each loading uncertainties, there may be some trade-off relations between robustness performances. Thus, some trade-off relations were investigated. In addition, relations between robust topologies and robustness performances are also investigated, because it is important to understand robust topologies characteristic.

5.1. Model of the lug structure and loadcases for multi-loadcase problem

The structural configuration of lug model and the design domain for topology optimization are shown in Fig. 5. The left-hand side (wing side) of model shown in a figure is fixed, and loadings are subjected through two pins of right-hand side (body side).

In this study, for simplicity, it is assumed that the bending moment and shear force are main reaction forces that receive from the main wing structure, and each loading uncertainties are independent. Each loading uncertainties assumed in this study are shown in Table 2, and six load cases are defined as shown in Fig. 6. for loading uncertainty. Magnitude and applied direction of each loadcase defined in this study are shown Table. 3. Loadcases 2, 3, 5, 6 are for the directional uncertainty.

In order to keep the constant magnitude of bending moment, regardless of pins y-position, the magnitude of the load case 1~3 was calculated by the magnitude received when pins position is 80mm away from the center height. The basic parameters of model are assumed to be E=113.8GPa, ν=0.3, density ρ=1, thickness t=1. The design domain was discretized into 40×50mesh.

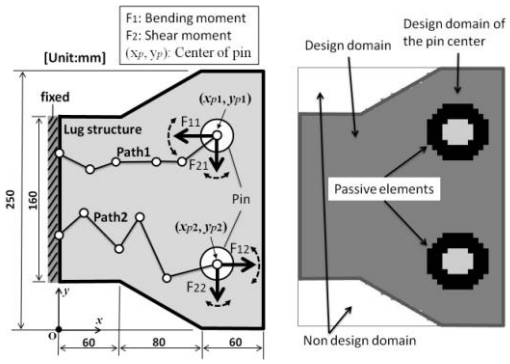

Figure 5: Lug structure model and design domain of the topology optimization

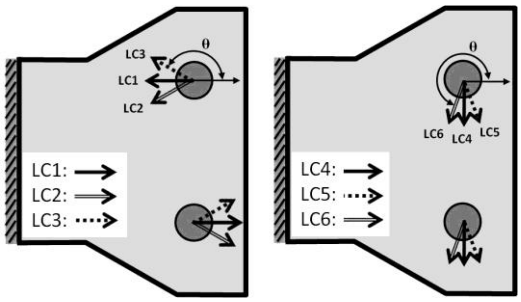

Figure 6: Loadcases of lug structure for robust topology optimization

Table 2: Loading uncertainty

	Bending moment		Shear force	
	Mean	Std	Mean	Std
Magnitude	$F_{11}(y_{p1}$=205mm)=80 $F_{12}(y_{p2}$= 45mm)=80	5	10	10
Direction(θ) [°]	θ_{11}=180, θ_{12}=0	40	270	20

Table 3: Magnitude and applied direction of each loadcases

No. Loadcase	Magnitude	Applied direction(θ)
1	$1 \cdot 80/\lvert y_p - 125 \rvert$	180°, 0°
2	$1 \cdot 80/\lvert y_p - 125 \rvert$	220°, -40°
3	$1 \cdot 80/\lvert y_p - 125 \rvert$	140°, 40°
4	1	270°
5	1	290°
6	1	250°

5.2. Multi-objective topology optimization using NSGA-IIa for multi-loadcase problem

Minimization of compliance problem with the multi-loadcase (Eq.1) was optimized by using NSGA-IIa. In this present study, population size of GA is 100 and all runs stopped after 800 generations in the GA, and Pareto-solutions are gathered from 5 independent runs.

For this topology optimization using GA, bar-system consist 2 paths of 5 bars (six vertexes) as shown Fig. 5. The positions of the left hand side vertices on the fixed boundary are variable along the clamped boundary support. The position of vertex on the center of pin is fixed at the loading point. In addition, in the topology optimization, position of pin center about y-axis was optimized as well as six vertexes of bar-system. Therefore, total number of variables in the present GA is 30. Each design variable ranges are as follows.

$$0 \le x_e \le 200, \quad 0 \le y_e \le 250, \quad 0 \le t \le 50$$

$$155 \le y_{p1} \le 220, \quad 30 \le y_{p2} \le 95$$

where t is the thickness of the edge of bars, x_e and y_e represent Cartesian coordinates of the point of the each edge of bar, respectively, and y_{pi} are the position of ith pin about y-axis. In addition, for simplicity of modeling between pin and lug structure, the passive element whose density is always 1 was set around pins instead of using some contact condition. Volume limit in Eq.(1) was set to correspond to 40% volume fraction.

The optimization result of NSGA-IIa is shown in Fig. 7. 674 Pareto-solutions in total were obtained. In the Fig.6, blue dots represent the feasible solutions, red dots represent Pareto-solutions, and a line which is made by red dots represents Pareto frontier. Compliance of each loadcase is represented in both axes.

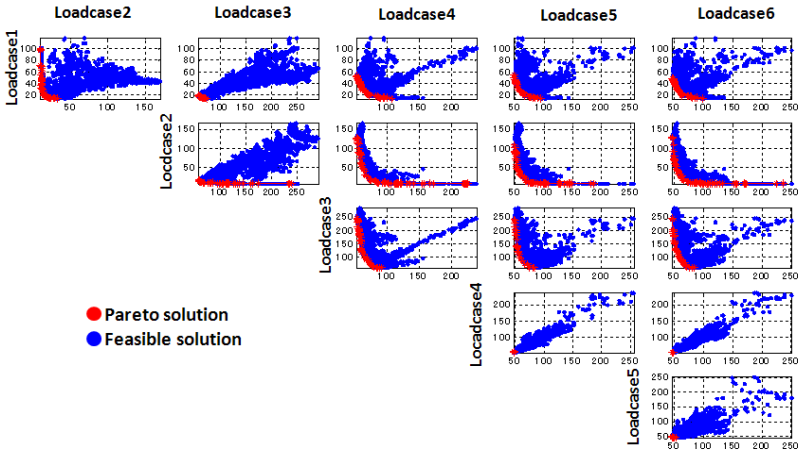

Figure 7: Objective space of compliance minimization problem with 6 loadcase of lug structure

5.3. Evaluation of the robustness performances of representative topologies

In order to reduce the computational cost, some representative topologies on the SOM were extracted, before the calculation of robustness performances. In this simulation, 311 representative topologies were extracted from the Pareto solutions of multi-loadcase problem. After that, all representative topologies were applied to Monte Carlo simulation according to the loading uncertainty (Table 1) with 10,000 load samples. The result is shown as Fig. 8. In this present study, we termed such Pareto-solutions obtained from a robustness performance space as "robust quasi-Pareto solutions".

In the Fig. 8, it is shown that there is no trade-off relation between EC_{Bend} (Expected compliance of bending moment) and $StdC_{Bend}$ (Standard deviation of compliance of bending moment) space, and between EC_{Shear} (Expected compliance of shear force) and $StdC_{Shear}$ (Standard deviation of compliance of shear force) space. This means that a topology whose low expected compliance has also low standard deviation of compliance. However, it is shown that there is strong trade-off relation between EC_{Bend} and EC_{Shear} space as shown Fig. 8. Thus, in loading uncertainty of lug structure, it is necessary to mainly explore the robust topologies in EC_{Bend} and EC_{Shear} space or $StdC_{Bend}$ and $StdC_{Shear}$ space.

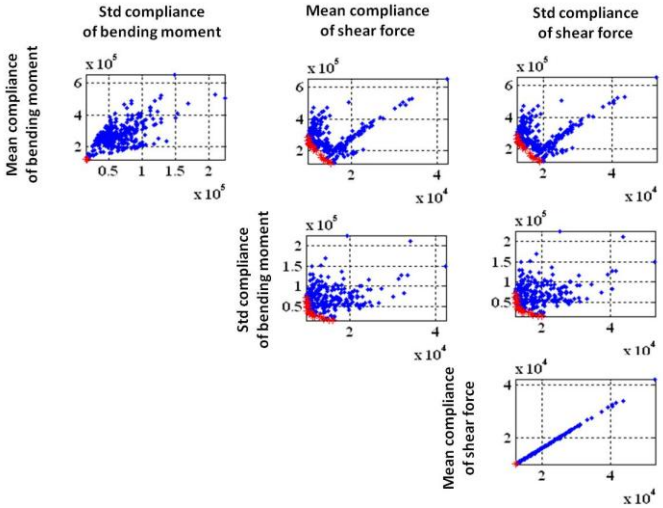

Figure 8: Robustness performance objective space

5.4. Exploration of robust lug topology using SOM

In present study, SOM was used in order to investigate efficiently about the relation between topology and robustness objectives. Results of classification of all Pareto-solutions obtained by NSGA-IIa and clustering are shown as Fig. 9. Topologies were classified according to some characteristics of topology defined above. Here, it is difficult to show all topologies on the each unit of SOM, only some topologies were shown. In Fig. 9(a), we can observe that adjacent individuals on the SOM have similar topology. In addition, SOM colored by similarity of

topology which is optimum topology of each loadcase are shown as Fig. 10. In Fig.10, units with red color (high similarity) mean that topology on the unit is similar to the topology above SOM, and those with blue color (low similarity) mean that topology on the unit is not similar to the topology above SOM.

Fig. 11 shows SOM colored by robustness performances such as EC_{Bend}, $StdC_{Bend}$, EC_{Shear} and $StdC_{Shear}$. First, SOM colored by EC_{Bend} and $StdC_{Bend}$ showed similar pattern in Fig. 11. It is suggests that EC_{Bend} and $StdC_{Bend}$ are not in a trade-off relation. In addition, EC_{Shear} and $StdC_{Shear}$ are not in a trade-off relation in the same manner. On the other hand, robustness EC_{Bend} and EC_{Shear} are in a trade-off relation because its SOM patterns show opposite color patterns. These results coincide with those of results of chapter 5.3. Moreover, by comparing the Figs. 9 and 11, it is clear that cluster 4 in lower right corner has small EC_{Bend} and $StdC_{Bend}$, and cluster 1 in upper left corner has small EC_{Shear} and $StdC_{Shear}$. This means that topologies in the cluster 4 are robust to bending moment uncertainty, and those in the cluster 1 are robust to shear force uncertainty.

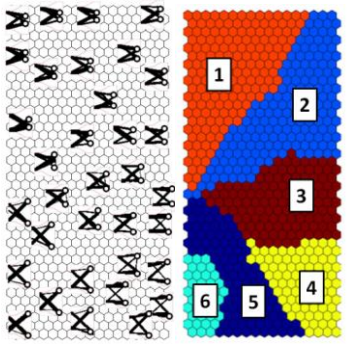

(a) (b)

Figure 9: (a) Topologies on the SOM and (b)result of clustering

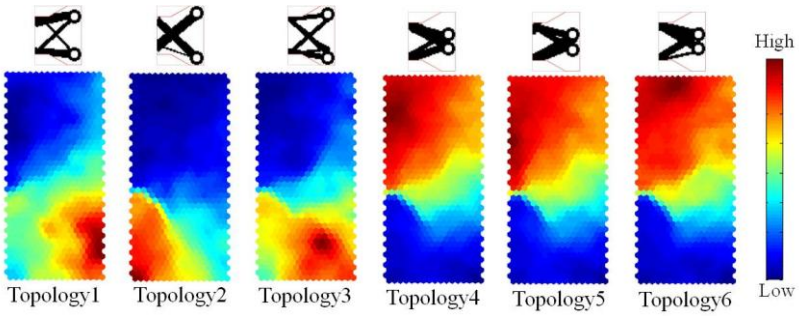

Figure 10: SOM colored by topology similarity to topology above SOM (Topology i (Optimum topology of ith loadcase))

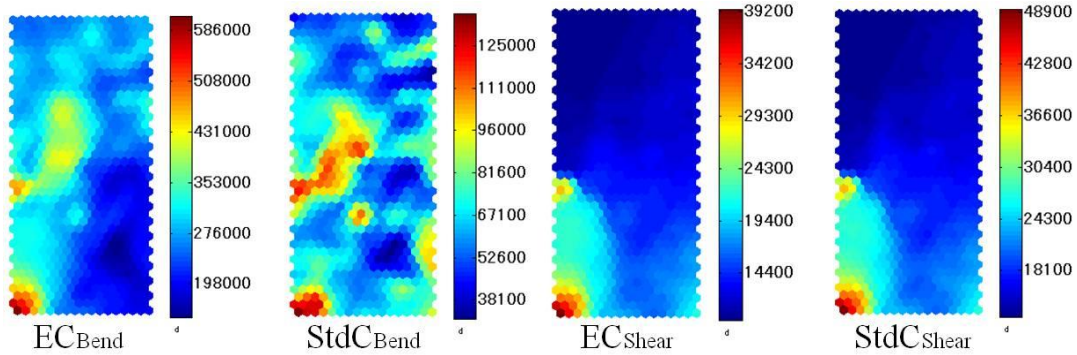

Figure 11: SOM colored by each robustness performances

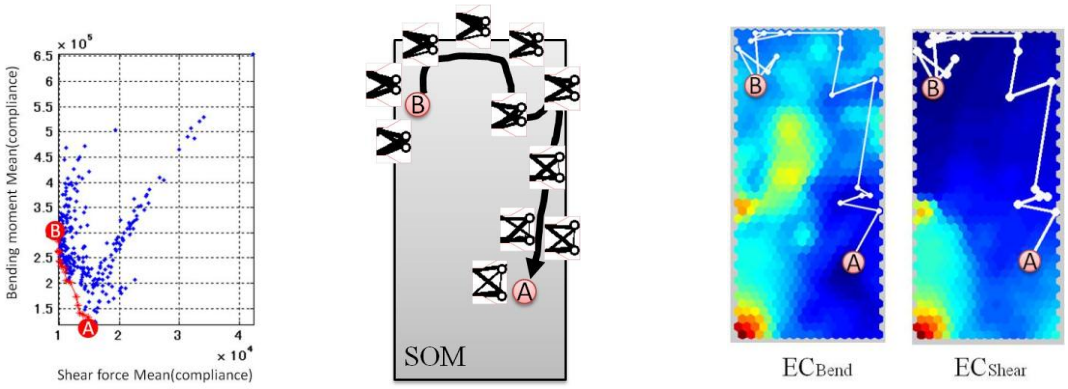

(a) (b) (c)

Figure 12: (a) Objective space of EC_{Bend} and EC_{Shear}, (b) Robust topologies on SOM, (c) Result of trajectory on SOM colored by EC_{Bend} and EC_{Shear}

By comparing Figs. 10 and 11, we find some relation between topology and robustness performances. Topologies with high similarity to the topology3 (optimum topology of loadcase 3) have high EC_{Bend} and $StdC_{Bend}$. In Fig. 10 of topology 1~3 SOM, we can find that topology 3 is located between topology 1 and topology 2 on SOM. It implies that topology 3 has both characteristics of topology 1 and 2. It is the reason why topology 3 is robust to bending moment uncertainty. In addition, topologies with high similarity to the topology4 (optimum topology of loadcase 4) have high EC_{Shear} and $StdC_{Shear}$. In Fig. 10 of topology 4~6 SOM, we can find that topology 4 is located between topology 5 and topology 6 on the SOM. It implies that topology 4 has both characteristics of topology 5 and 6. It is the reason why topology 4 is robust to shear force uncertainty.

In order to investigate the robust topologies in the EC_{Bend} and EC_{Shear} space, where strong trade-off relation was shown, individuals between A to B of Fig. 12(a) was shown in Fig. 12(b). In addition, trajectory from A to B was plotted on the EC_{Bend} and EC_{Shear} of SOM in Fig. 12(c). As shown in Figs. 12(b) and 12(c), the robust quasi-Pareto solutions are located from the cluster 1 to 4 in order. Moreover, topologies in the clusters 2, 3 have balanced performance of expected compliance and variance. Moreover, we can find that topologies in the cluster 2, 3 have both characteristics of topology 1 and 4 by comparing Figs. 10 and 12(b).

6. Conclusions

In this present study, for the robust topology optimization of lug structure with loading uncertainty, Multi-Objective Genetic Algorithms was used with multi-loadcases problem. And for the efficient exploration of the robust topology in the objective space, exploration method by using SOM was proposed, and applied to lug structure design problem. SOM shows effectively some trade-off relations between objective functions, in addition, relations between topologies and objective functions.

7. References

[1] Achtziger, W., Topology optimization of discrete structures: an introduction in view of computational and nonsmooth aspects. In: Rozvany, G.I.N (ed.) *Topology Optimization in Structural Mechanics*, Springer-Verlag, New York, 1997.

[2] Calafiore, G. C., and Dabbene, F., Optimization Under Uncertainty with Applications to Design of Truss Structures, *Structural and Multidisciplinary Optimization*, 35 **(**3), 189–200, 2008.

[3] Conti, S., Held, H., Pach, M., Rumpf, M., and Schultz, R., Shape Optimization Under Uncertainty: A Stochastic Programming Perspective, *SIAM Journal on Optimization*, 19 (4), 1610–1632, 2009.

[4] Kohonen, T.: *Self-Organizing Maps*, Springer, 105-116, 2001.

[5] Welch W.J., Buck R.J., Sacks J., Wynn H.P., Mitchell T.J., and Morris M.D., "Screening, Predicting, and Computer Experiments", *Technometrics*, 34 (1), 15-25, 1992.

[6] Deb, K., Agrawal, S., Pratap, A., Meyarivan, T., A fast and elitist multi-objective genetic algorithm for multi-objective optimization: NSGA-II, in: *Proceedings of the Parallel Problem Solving from Nature VI Conference*, Paris, 849-858, 2000.

[7] Goel, T., Vaidyanathan, R., Haftka, R. T., Shyy, W., Queipo, N. V. and Tucker, K., Response surface approximation of Pareto optimal front in multi-objective optimization, *Computer. Methods Applied Mechanics and Engineering*., 196, 879 -893, 2007.

[8] Wang, S. Y. and Tai, K., Bar-system representation method for structural topology optimization using the genetic algorithms, *Engineering Computations*, 22-2, 206-231, 2005.

[9] Deb, K., Anand, A., Joshi, D., A computationally efficient evolutionary algorithm for real-parameter optimization, *Evolutionary Computation*, 10-4, 371–395, 2002.

[10] Deb, K. and Goyal, M., A combined genetic adaptive search (GeneAS) for engineering design, *Computer Science and Informatics*, 26-4, 30–45, 1996.

[11] Vesanto J., Himberg J., Alhoniemi E., Parhankangas J.: SOM Toolbox for Matlab 5, available at http://www.cis.hut.fi/projects/somtoolbox/, (Last accessed: 17 December 2012)

[12] Vesanto J., Alhoniemi E., Clustering of the Self-Organizing Map, *IEEE Transactions on neural Networks*, 11-3, pp.586-599, 2000.